Case Studies in Construction Materials 19 (2023) e02227

Contents lists available at ScienceDirect

Case Studies in Construction Materials

journal homepage: www.elsevier.com/locate/cscm

Experimental investigation and analytical prediction of flexural behaviour of reinforced concrete beams with steel fibres extracted from waste tyres

Sadık Alper Yıldızel [a], Yasin Onuralp Özkılıç [b,*], Alireza Bahrami [c,*], Ceyhun Aksoylu [d], Boğaçhan Başaran [e], Ahmad Hakamy [f], Musa Hakan Arslan [d]

[a] Civil Engineering Department, Faculty of Engineering, Karamanoglu Mehmetbey University, Karaman, Turkey
[b] Department of Civil Engineering, Faculty of Engineering, Necmettin Erbakan University, Konya 42000, Turkey
[c] Department of Building Engineering, Energy Systems and Sustainability Science, Faculty of Engineering and Sustainable Development, University of Gävle, 801 76 Gävle, Sweden
[d] Department of Civil Engineering, Faculty of Engineering and Natural Sciences, Konya Technical University, Konya 42250, Turkey
[e] Department of Construction, Vocational School of Technical Sciences, Amasya University, Amasya 05100, Turkey
[f] Department of Physics, Faculty of Applied Science, Umm Al-Qura University, Makkah 21955, Saudi Arabia

ARTICLE INFO

Keywords:
Recycled
Reinforced Concrete Beam
Scrap
Steel
Tyre
Waste
Wire

ABSTRACT

In recent years, studies on the use of car tyre wastes in concrete have gained momentum. Especially, the effect of recycled waste steel wires (RWSWs) from tyres to be mixed into concrete for using in newly designed reinforced concrete buildings on the performance of construction elements is a fairly new research area. In this study, the bending behaviour of 12 reinforced concrete beams was investigated having 1/3 geometric scale, 100 × 150 × 1000 mm in size, and produced with RWSWs additive in different volumetric ratios (1%, 2%, and 3%) under vertical loads. Another main parameter selected in the study was the amount of varying tension reinforcements (2ϕ12, 2ϕ10, and 2ϕ8). The load-carrying, stiffness, ductility, and energy dissipation capacities of the RWSW reinforced bending beams were compared with the primary aim of this study which was to examine and present the contribution of RWSWs on the improvement of the bending performance of the reinforced concrete beams. The results revealed that the mechanical properties of the hybrid beams with RWSWs vary depending on dosages but are comparable with those of the beams-only with the same fibre dosage. A positive effect was obtained for the hybrid beams containing 2–3% RWSWs. Besides, RWSWs were found to be highly well mobilised at larger crack widths, and the post-cracking strength of RWSW mixes was significantly higher. Considering both mechanical properties of the beams and fresh properties such as the workability, 2% of RWSWs is recommended to be utilised in the reinforced concrete beams. On the other hand, the results were compared with the predictions of the methods given in the literature and standards. Moreover, an equation was derived to better predict the capacity of the hybrid beams using RWSWs.

* Corresponding authors.
E-mail addresses: yozkilic@erbakan.edu.tr (Y.O. Özkılıç), alireza.bahrami@hig.se (A. Bahrami).

https://doi.org/10.1016/j.cscm.2023.e02227
Received 15 April 2023; Received in revised form 23 May 2023; Accepted 19 June 2023
Available online 19 June 2023

1. Introduction

In order for the ductile power depletion to occur in a reinforced concrete element, the longitudinal reinforcement ratio must be well under the balanced reinforcement ratio (ρ_b) and there must be sufficient stirrup reinforcements to prevent the shear damage. When these conditions are met, the reinforced concrete element can only reach its bending capacity through moment. Theoretically, it does not have a significant effect on the bending capacity of beams, especially where the axial force level is lower since the tensile strength of concrete is quite low. However, the increasingly difficult access to raw materials in the world has led to an increase in new searches [1–5]. Moreover, increasing global warming with industrialisation, and sustainability concerns with ecological approaches have also played role in this issue [6]. For this reason, innovative techniques have become an important research topic as they use fewer raw materials and become more eco-friendly materials [7–11]. In addition, some of the investigations are utilised to increase the very weak tensile strength of concrete via eco-friendly solutions [12–16].

In the studies carried out in the last decade, natural fibres, metallic (steel), synthetic (polymers) and mineral (carbon or glass) fibres, chemical agents, etc., have been widely used to increase and strengthen the tensile strength of concrete [17]. Apart from them, the evaluation of the materials obtained by recycling industrial fibre wastes, which have become popular in recent years, in concrete has great importance in the context of sustainability.

There are many studies in the literature involving different fibrous materials [18–22]. Steel, polypropylene, carbon, plant, and alkali-resistant glass fibres are commonly used fibres in concrete [23–27]. Steel fibres are the most widely employed fibre type, thanks to the superior mechanical properties they impart to concrete. It is also possible to classify these fibre types according to their geometric properties [28]. Accordingly, the cross-sections of fibres may be round or flat (such as plaque), as well as different types of steel fibres in terms of surface shapes and geometric forms [28]. In addition to the geometric difference, the length/diameter (l/d, slenderness λ) ratios of steel fibres are very important [29]. Steel fibres can have normal (low carbon) or high (high carbon) strength properties according to the carbon they contain. In fibrous concretes, the most important feature that must be provided in all fibre types is that fibres are distributed homogeneously in concrete and this distribution does not deteriorate after concrete is mixed.

The main purpose of steel fibre reinforcement in concrete is to increase the tensile and compressive strengths of brittle concrete, which contains numerous micro-cracks, and to increase the deformation capacity (in other words, the very limited ductility of concrete). Steel fibres cause an increase in the ductility and tensile strength of the material by delaying the formation of cracks in concrete or preventing the cracks propagation (bridging) under stresses [30]. Thus, the deformation capacity and the toughness of steel fibre concrete, whose tensile strength increases compared with conventional concrete, also increase [31–33]. In this case, it is possible to say that the sections of the structural elements can be dimensioned economically when used with fibre reinforced concrete reinforcements, especially where bending is effective. There is no definite consensus in the literature about the effect of steel fibres on the compressive strength of concrete. But it is obvious that it improves the tensile strength. Because when the axial tensile stresses, which are the main cause of cracking in concrete, act in the direction of fibres, after concrete cracks, fibres come into play and additional strength is gained. This situation has been studied by many researchers. Bonakdar et al. [34] stated that with the addition of steel fibres, the post-crack response of concrete can be changed from brittle to ductile under various loads including compression, tension, bending and impact. Buratti et al. [35] showed that steel and synthetic macrofibres significantly enhance the post-crack response of concrete and provide residual strength values that can be used for design purposes.

Apart from these methods, recycled steel fibres derived from waste tyres have come to the fore as an alternative to steel fibres in recent years. Especially, the rapid development of the automotive industry has given birth to many new projects about the disposal of waste tyres [36–38]. How to recycle and dispose waste tyres reasonably and effectively, which has become a problem in developed countries, and how to prevent environmental pollution, have become a problem that people have to face.

There are many investigations on the strength features of concrete with steel scrap and also there are several studies on the performance of concrete with steel wastes in the literature [39–44]. However, in the literature, research works on the impacts of different proportions of waste tyre fibres on the bending behaviour are still insufficient. Consequently, influence of steel fibres extracted from waste tyres on the flexural behaviour of reinforced concrete beams is an important topic.

Around the world, approximately 1–1.5 billion tyres have completed their useful life, and it is estimated that this number will approach approximately 5 billion by 2030 [45,46]. These tyres are usually deposited or incinerated at stockpiles. This situation raises the problem of storage of waste tyres [47–50]. There are many ways to recycle this waste without harming the environment; one of them is incineration in cement kilns and the other is that it is added to concrete as both aggregate and binder. In particular, recycled waste steel wires (RWSWs) from tyres are added to concrete and contribute to the improvement of the mechanical properties of concrete [51–53]. Wang [20] paved the way for recycling by reporting that industrial waste fibres and original fibres have the same effect. Neocleous et al. [54] obtained a rather interesting result. They demonstrated that RWSWs caused a significant improvement in the behaviour of concrete after the maximum stress. This situation has also indicated that the sudden decrease in the load capacity after the maximum stress, which is the most important disadvantage of concrete, can be delayed with RWSWs. Aiello et al. [55], Yang et al. [56], and Kamran and Mohammad [57] have mentioned that RWSWs have micro-reinforcement feature for reinforced concrete.

These pioneering studies have encouraged the use of tyre recycling in civil engineering. Many studies in the literature have been evaluated in this context. Koroglu and Ashour [58] stated that RWSWs, which are added to self-compacting concrete at the rates of 4% and 5%, increase the bending capacity of beams by 6 times. Several investigations illustrated that RWSWs reduce the compressive strength of concrete [59,60]. However, some studies revealed that RWSWs improve the compressive strength [42,61,62]. In recent years, research has been carried out to assess the contribution of RWSWs to the shear capacity of beams. Aksoylu et al. [42] investigated the contribution of 1%, 2%, and 3% of RWSWs to small scale shear beams according to different stirrup spacings. It was stated in this study that although the effect of fibre content in specimens with high stirrup spacing (27 cm) provides significant benefit in

Fig. 1. RWSWs used for experiments.

Fig. 2. Preparation of beams.

improving the beam's behaviour, the effect of fibres is more limited as the stirrup spacing decreases (20 cm and 16 cm).

By examining the literature, it is understood that addition of steel fibres has a positive effect on the mechanical properties of concrete. However, when limited resources and sustainability are considered, research on materials such as RWSWs becomes very valuable. The importance of this study is that the load-carrying, stiffness, ductility, and energy dissipation capacities of RWSW reinforced bending beams are compared experimentally. In order to make these comparisons, an experimental program was created, and the outputs were presented. The bending behaviour of 12 small-scale rectangular simply supported reinforced concrete beams (100 × 150 × 1000 mm) was investigated under vertical loads, which were produced with RWSWs additive in different volumetric ratios (0%, 1%, 2%, and 3%). Another main parameter selected was the amount of varying tension reinforcements (2ϕ12, 2ϕ10, and 2ϕ8). Compression reinforcements were kept constant as 2ϕ6 since they do not have a significant effect on the bending capacity. Furthermore, a constant stirrup spacing of 100 mm was taken into account due to the fact that the bending capacity and ductility of the beams were examined in the experimental program. The experiments were conducted with a four-point bending test machine.

2. Materials and method

2.1. Mixture design and specimen preparation

As it was mentioned, RWSWs were utilised in this experimental study. The used RWSWs are displayed in Fig. 1. RWSWs were divided into small pieces before the mixing process. The average length of RWSWs was approximately 30–50 mm. RWSWs longer than 100 mm were not employed to avoid aggregation. CEM I 32.5 type of Portland cement conforming to the EN 197–1 standard was also used. The water–cement ratio was selected as 0.6 for all the mixtures. RWSWs were added to the mixture slowly to avoid aggregation during the mixing process. The mixture was poured into the moulds in the small amounts to ensure the best compatibility of concrete. Compaction was also applied with the help of a vibrator. Cylinder and cube samples were produced for the mechanical tests. The preparation steps are depicted in Fig. 2.

10 × 20 cm cylinder and 15 × 15 × 15 cm cube samples were used for the compressive and splitting tensile strengths tests according to the EN 206 and ASTM D3967 standards, respectively. The cylinder and cube average compressive strengths were obtained

Table 1
Details of specimens.

Number	Specimen Name	Stirrup (mm)	Longitudinal Reinforcement		V_f
			Compression Reinforcement	Tension Reinforcement	
1	BREF-1	ϕ6/100	2ϕ6	2ϕ12	0%
2	BTYRE-1	ϕ6/100	2ϕ6	2ϕ12	1%
3	BTYRE-4	ϕ6/100	2ϕ6	2ϕ12	2%
4	BTYRE-7	ϕ6/100	2ϕ6	2ϕ12	3%
5	BREF-2	ϕ6/100	2ϕ6	2ϕ10	0%
6	BTYRE-2	ϕ6/100	2ϕ6	2ϕ10	1%
7	BTYRE-5	ϕ6/100	2ϕ6	2ϕ10	2%
8	BTYRE-8	ϕ6/100	2ϕ6	2ϕ10	3%
9	BREF-3	ϕ6/100	2ϕ6	2ϕ8	0%
10	BTYRE-3	ϕ6/100	2ϕ6	2ϕ8	1%
11	BTYRE-6	ϕ6/100	2ϕ6	2ϕ8	2%
12	BTYRE-9	ϕ6/100	2ϕ6	2ϕ8	3%

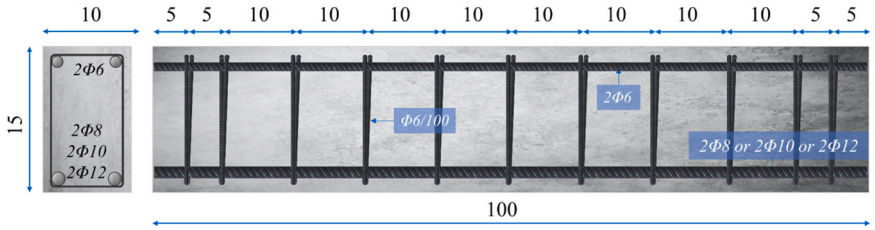

Fig. 3. Reinforcements layout (dimensions are in cm).

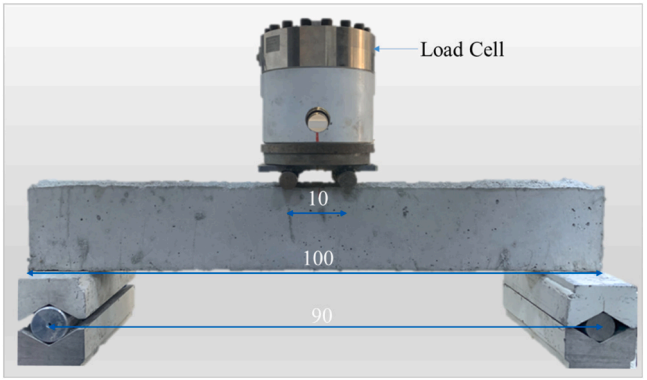

Fig. 4. Test setup (dimensions are in cm).

as 25 MPa and 29.5 MPa, respectively, for concrete without any RWSWs, as expected. Besides, the compressive strengths of 29 MPa (cylinder) and 34.6 MPa (cube) for 1% RWSWs content, 32 MPa (cylinder) and 38.6 MPa (cube) for 2% RWSWs content, and 37 MPa (cylinder) and 43.2 MPa (cube) for 3% RWSWs content were also noted. The splitting tensile strengths were achieved as 2.83 MPa for the reference sample, and 3.24 MPa, 3.54 MPa, and 3.87 MPa respectively for the samples containing 1%, 2%, and 3% RWSWs. In the literature [63], when the conversion coefficients (0.738 and 0.96) were applied for the standard cube (15 × 15 × 15 cm) and standard cylinder (15 × 30 cm), the compressive strength of the reference sample and the samples with 1% RWSWs content, 2% RWSWs content, and 3% RWSWs content was calculated as 21.7 MPa, 25.53 MPa, 28.48 MPa, and 31.88 MPa, respectively. In this way, 10 × 20 cm cylinder and 15 × 15 × 15 cm cube samples used in the experiments were expressed as standard cubes (15 × 15 × 15 cm) and cylinders (15 × 30 cm).

A total of 12 specimens were manufactured. The primary variable of the study was the volume fraction of RWSWs. Four different fibre ratios of 0%, 1%, 2%, and 3% were utilised by volume. The second variable was longitudinal reinforcements. Three different longitudinal reinforcements of 2ϕ8, 2ϕ10, and 2ϕ12 were employed. Table 1 presents details of the specimens. In the table, V_f is the volume fraction of fibres (RWSWs).

Table 2
Experimental results for load and displacement values.

Test Specimens	P_{max} (kN)	Displacement at P_{max} (mm)	Rigidity at P_{max} (kN/mm)	P_u (0.85P_{max}) (kN)	Displacement at P_u, δ_y (mm)	Rigidity at P_u (kN/mm)	δ_u (mm)	Ductility Ratio
BREF-1	51.91	5.58	9.31	44.13	2.45	18.05	14.71	6.02
BTYRE-1	60.65	8.06	7.53	51.55	3.91	13.18	12.38	3.16
BTYRE-4	62.33	10.48	5.95	52.99	4.05	13.08	18.20	4.49
BTYRE-7	63.47	9.89	6.42	53.96	4.21	12.82	21.56	5.12
BREF-2	45.29	10.59	4.28	38.50	2.51	15.35	24.62	9.82
BTYRE-2	48.68	40.67	1.20	41.39	2.21	18.70	57.37	25.92
BTYRE-5	48.56	40.72	1.19	41.28	2.71	15.23	64.58	23.83
BTYRE-8	48.48	37.36	1.30	41.22	3.34	12.35	85.86	25.73
BREF-3	35.44	12.46	2.84	30.13	0.83	36.51	66.32	80.38
BTYRE-3	36.85	4.02	9.16	31.33	1.71	18.35	66.27	38.81
BTYRE-6	36.76	47.78	0.77	31.25	2.32	13.49	65.92	28.46
BTYRE-9	36.99	42.48	0.87	31.45	2.37	13.26	66.63	28.10

2.2. Test set up and reinforcements details

The beam specimens used in the study have widths (b_w) of 100 mm, heights (h) of 150 mm, and lengths (L) of 1000 mm. In all the specimens, 6 mm diameter stirrups were placed at 100 mm intervals to prevent any shear collapse that might occur in the beams. The stirrups have been confined to prevent compression damage in the support region. The reinforcements layout is illustrated in Fig. 3, and the test setup is displayed in Fig. 4.

3. Experimental results and discussion

Displacements and rigidities at the maximum load (P_{max}) and 0.85 P_{max} (P_u) are given in Table 2. The 0.85 P_{max} value was determined on the curve where the load-displacement curve reached the maximum load. Compared with BREF-1, P_{max} of BTYRE-4 and BTYRE-7 increased by 20.1% and 22.3%, respectively. The RWSWs inclusion up to 3% improved the maximum and ultimate loads at similar intervals. From Table 3, it can also be seen that the P_{max} test results of BTYRE-5 and BTYRE-8 were increased by 7.0% and 7.2%, respectively, compared with that of BREF-2. When the third group is examined, it is observed that the increasing trend decreased to 4%. This situation can be attributed to the decreasing tension reinforcement contents of the beams [64,65]. RWSWs can be efficiently utilised with the tension bar of ϕ12. Furthermore, the addition of RWSWs led to the reduction of stresses during the crack forming and propagation since they acted as the load-transferring elements [66–68]. The rigidities generally tended to decrease depending on the amount of RWSWs, and the obtained results are compatible with similar literature studies [47,69].

Total energy dissipation of the beams can largely affect the damage level and related deformations during earthquakes when the sufficient ductility level is provided by these members. The experimental tests results for the energy dissipation capacities of the elements are presented in Table 3. BTYRE-8 demonstrated the maximum total energy dissipation of 3.94 kJ during the test procedure. The test results of BREF-1 and BTYRE-1 were obtained as out of the limits concerning their ductility levels. When the other two specimens in the first group are examined, it is witnessed that partially acceptable results have been achieved. In general, the RWSWs inclusion increased both the ductility levels and energy dissipation capacities due to their stress reduction effects [70–72]. The literature suggests that the ductility ratio (ductility coefficient) should be around 4 ~ 5 for a sub-balanced ductile design [73,74]. It is evidenced from Table 2 and the load-displacement curves of the specimens that the ductile behaviour was achieved.

The ultimate damage patterns of BREF-1, BTYRE-1, BTYRE-4 and BTYRE-7 are shown in Fig. 5. The failure type of BREF-1 and BTYRE-1 was similar, and their shear resistances were lower than their flexural strengths due to their low RWSWs contents and insufficient shear reinforcements [75,76]. The failure characteristics of BTYRE-4 and BTYRE-7 exhibited that RWSWs were forced to carry loads after the yield of steel reinforcements, which implied that RWSWs in this beam could effectively bear parts of the shear forces. Meanwhile, the failure pattern of BTYRE-7 also indicated that RWSWs bundle was not uniform, and some parts of the beam failed early. Figs. 6 and 7 display the failure types of the second and third groups of the beams. The experimental tests results revealed that both groups were failed by the bending effects. However, some cracks were also formed owing to the shear forces [77,78], especially for the beams with no and low RWSWs content.

The load-displacement curves of the 12 composite beams are presented in Fig. 8. Compared with the other specimens, the beams with high RWSWs contents had the maximum displacement results. BREF-2 illustrated less displacement result among all the beams. Moreover, curves of all the beams in each group were observed to have similar characters especially for the elastic stage [79]. However, the displacements of the beams with 2% and 3% RWSWs contents were greater than the reference beams.

It can be concluded that the RWSWs inclusion has a noticeable effect on the mid-span displacements. Fig. 8 also depicts that the flexural stiffness of the specimens decreased owing to lower modulus of elasticity. On the other hand, it can be seen that adding 3% RWSWs escalated the ultimate deflection capacity. For BTYRE-8, it was obtained as 85.87 mm. RWSWs can take more tension and resist deformations by bridging the local stresses [80–82]. In addition, increasing the RWSWs ratio decreased the workability; after 2% RWSWs ratio, the workability considerably dropped.

Table 3
Experimental results for energy dissipation capacities.

Test Specimens	Maximum Displacement (mm)	Energy Dissipation at P_{max} (kJ)	Energy Dissipation at P_u (kJ)	Plastic Energy Dissipation (kJ)	Total Energy Dissipation (kJ)	Failure Type	Ductility Level
BREF-1	23.68	0.21	0.06	0.95	1.01	Shear	Deficient
BTYRE-1	28.10	0.37	0.13	1.06	1.19	Shear	Deficient
BTYRE-4	27.96	0.52	0.14	1.28	1.41	Bending	Partially Sufficient
BTYRE-7	27.95	0.68	0.14	1.31	1.46	Bending	Partially Sufficient
BREF-2	28.24	0.41	0.05	1.08	1.13	Bending	Sufficient
BTYRE-2	62.00	1.86	0.05	2.77	2.82	Bending	Sufficient
BTYRE-5	64.91	0.00	0.05	2.91	2.96	Bending	Sufficient
BTYRE-8	85.87	1.68	0.07	3.88	3.94	Bending	Sufficient
BREF-3	66.40	0.40	0.01	2.20	2.22	Bending	Sufficient
BTYRE-3	67.00	0.12	0.03	2.32	2.35	Bending	Sufficient
BTYRE-6	66.74	1.68	0.08	2.26	2.34	Bending	Sufficient
BTYRE-9	66.73	1.45	0.04	2.30	2.34	Bending	Sufficient

Fig. 5. Failure patterns of tested beams – I.

Fig. 6. Failure patterns of tested beams – II.

4. Effect of RWSWs on tensile and flexural capacities of concrete

The tensile stress of concrete and the contribution of RWSWs to the tensile stresses are summed up in the ratio of the volumes of the materials when calculating the maximum tensile strength of RWSW concrete (Eq. 1) [83,84]. Similarly, in this study, Eq. 2 can be derived by using the empirical equations and general equations to determine the tensile stress of concrete reinforced with RWSWs. Eqs. 2 and 3 were utilised to determine the bending tensile strength of concrete (f_r) ACI 318–19 [85].

$$\sigma_{cc} = \sigma_c\left(1 - V_f\right) + \sigma_f V_f \tag{1}$$

Fig. 7. Failure patterns of tested beams – III.

$$f_{sfr} = f_r\left(1 - V_f\right) + \sigma_f V_f \tag{2}$$

$$f_r = 0.62\sqrt{f_c'} \tag{3}$$

where σ_{cc} is the tensile strength of composite material (MPa), σ_c is the tensile strength of concrete (MPa), σ_f is the pull-out strength of fibre (MPa), V_f is the fibre volume fraction, f_{sfr} is the tensile strength of fibre reinforced concrete (MPa), f_r is the modulus of rupture (MPa), and f_c' is the concrete cylinder compressive strength (MPa). Further, in order to determine the effect of the RWSWs additive on the tensile capacity of concrete, the bond between fibre and concrete is used (Fig. 9). The tensile force that a single fibre can bear and the average number of fibres per unit area are calculated using Eqs. 4 and 5, respectively. The total stress carried by fibres at the moment when they are stripped from concrete is calculated by Eq. 6.

$$F_t = \tau\pi d\frac{l}{2} \tag{4}$$

$$n = \frac{4V_f}{\pi d^2} \tag{5}$$

$$\sigma_t = nF_t = 2\alpha\tau V_f\frac{l}{d} \tag{6}$$

$$\sigma_f = 2\alpha\tau\frac{l}{d} \tag{7}$$

where τ is the bond strength of fibres (MPa), n is the average number of fibres per unit area, F_t is the pull-out force that a single fibre can carry (N), σ_t is the pull-out strength (residual tensile strength) of fibres (MPa), α is the fibres' efficient coefficient depending on the their diameter, length, shape, angle, group effect, etc.

To determine the contribution of steel fibres to the tensile stress (σ_t) of concrete, regulations and researchers have derived various equations. These equations are arranged for plain straight fibres and provided in Table 4.

where f_{ck} is the cube compressive strength of concrete at 28 days, F_{be} is the bond efficiency of fibres which can be considered from 1.0 to 1.2, β is the bond factor that can be taken equal to 0.50 for round fibres according to Campione et al. [90], and f_{cf} is the compressive strength of steel fibre reinforced concrete (MPa).

In the present study, the equivalent rectangular stress distribution model proposed in ACI 318–19 [85] was used to calculate the bending capacities of normal concrete beams. Singh [86] stated that the strain and stress distributions in the compressive and tensile zones formed in the steel fibre reinforced concrete (SFRC) beam sections can be as in Fig. 10a and b, respectively. In Fig. 10, A_s is the area of the tension reinforcement, A_s' is the area of the compression reinforcement, d' is the distance between the centre of the

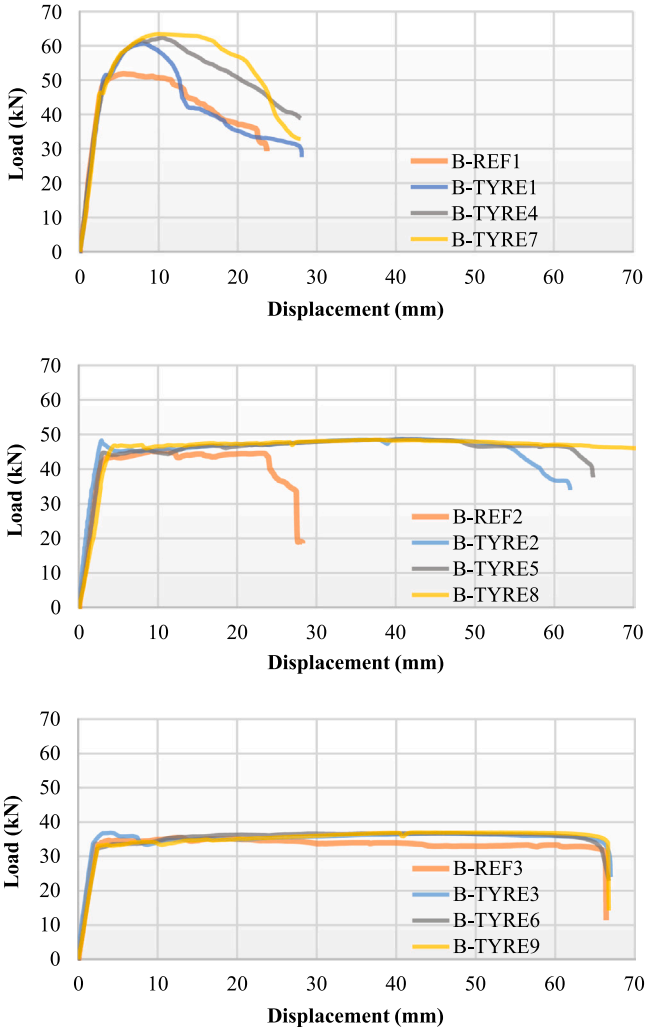

Fig. 8. Load-displacement (mid-span) relations of beams.

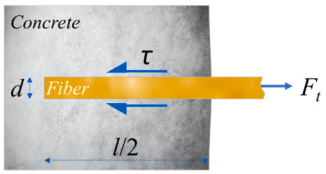

Fig. 9. Bond between RWSW and concrete.

compression reinforcement and the outermost concrete fibre, c is the distance of the neutral axis, d is the effective depth of beam, c_b is the concrete cover, u_{cr} is the uncracked section, ε_{cu} is the strain of the outermost concrete fibre, ε_s' is the strain of the compression reinforcement, ε_s is the strain of the tension reinforcement, β_1 is the depth coefficient of the equivalent stress block, k_3 is the coefficient of the equivalent compression stress block, F_s' is the compression reinforcement force, F_c is the concrete compressive force, F_{uc} is the uncracked concrete tensile force, F_{sfr} is the pull-out force of steel fibres, and F_s is the tension reinforcement force.

In order to calculate the bending capacities of the beams with RWSWs, some assumptions were made in this model, and the strain-stress model was idealized as in Fig. 10c. These assumptions can be listed as follows:

- An equivalent rectangular stress block is formed in the compression region of the beam. However, the coefficient of the equivalent compression stress block (k_3), which is 0.85 in normal concrete, increases to 0.95 at the time of failure in SFRC concrete [91].

Table 4
Pull-out strength of fibres for plain straight steel fibre reinforced concrete.

References	Equation
Singh [86]	
	$\sigma_t = 0.3V_f\frac{l}{d}\sqrt{f_{ck}}$ (8)
ACI 544.4 R [87]	
	$\sigma_t = 0.772V_f\frac{l}{d}F_{be}$ (9)
Campione [88]	
	$\sigma_t = 0.2V_f\frac{l}{d}\beta\sqrt{f_{cf}'}$ (10)
Beshara et al. [89]	
	$\sigma_t = 1.64V_f\frac{l}{d}$ (11)

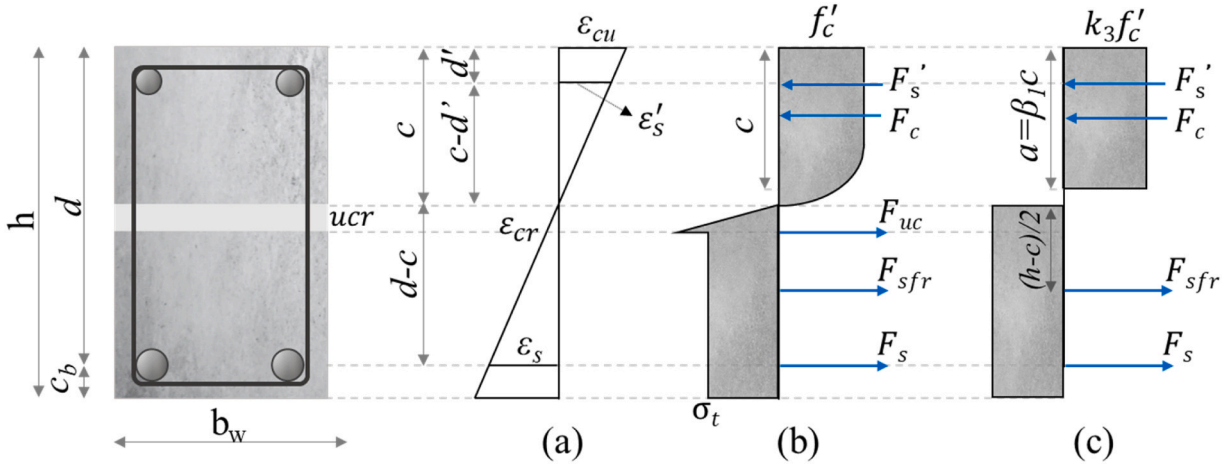

Fig. 10. SFRC beam section subjected to bending: (a) Strain distribution; (b) Stress distribution; (c) Idealized stress distribution.

- The depth of the equivalent stress block varies according to the compressive strength of concrete ($\beta_1 c$). The suggested coefficients of ACI 318–19 [85] are utilised.
- While the final unit strain (ε_{cu}) of concrete is usually 0.003 in normal concrete, it can be up to 0.004 in SFRC concrete [86,92].
- In the beam tension zone, the effect of concrete on the tensile propagation is up to the initial cracking of the beam. Also, concrete demonstrates no shrinkage effect after the first crack initiation in the beam.
- The effect of RWSWs on the tensile behaviour is continuous. The contribution of RWSWs to the tensile stress is assumed to be an equivalent rectangle from the outermost fibre to the neutral axis.

Axial equality (Eq. 12) and conformity (Eq. 13) equations were utilised to calculate the bending capacities of the beams with normal concrete and RWSW concrete. Using these equations, the equation of the neutral axis depth, Eq. 14, was derived. Then, the bending capacity of the beams (M_n) was calculated employing Eq. 15.

$$F_s + F_{sfr} = F_c + F_s^{'} \tag{12}$$

$$\sigma_s^{'} = \varepsilon_{cu}E_s^{'}\frac{c-d^{'}}{c} \tag{13}$$

$$c = \frac{A_s f_y + \sigma_t b_w h - A_s^{'}\left(\varepsilon_{cu}E_s^{'}\frac{c-d^{'}}{c}\right)}{k_3 f_c^{'} b_w k_1 + \sigma_t b_w} \tag{14}$$

Table 5
α coefficients determined according to experimental results.

Test Specimens	$(\rho\text{-}\rho')V_f$	α	σ_t (MPa)	$P_{Exp.}$ (kN)
BTYRE-1	0.0001305	9.98	0.70	60.65
BTYRE-4	0.0002610	6.72	0.99	62.33
BTYRE-7	0.0003915	4.44	1.06	63.47
BTYRE-2	0.0000773	16.96	0.71	48.68
BTYRE-5	0.0001547	6.58	0.58	48.56
BTYRE-8	0.0002320	2.98	0.42	48.48
BTYRE-3	0.0000338	26.36	0.48	36.85
BTYRE-6	0.0000677	10.27	0.39	36.76
BTYRE-9	0.0001015	5.70	0.35	36.99

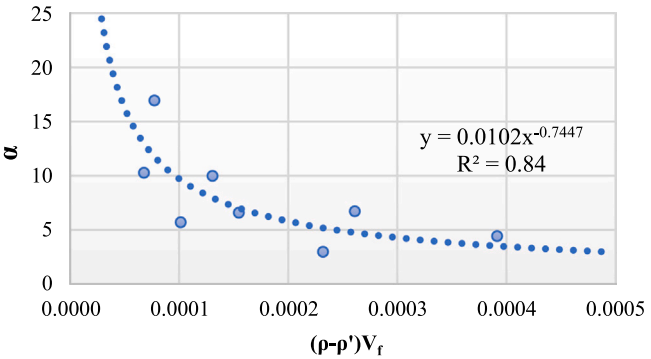

Fig. 11. Variation of α coefficients $(\rho\text{-}\rho')$ with respect to V_f.

$$M_n = A_s f_y\left(d - \frac{k_1 c}{2}\right) + \sigma_t b_w (h-c)\left(\frac{h + c - k_1 c}{2}\right) + A_s^{'}\sigma_s^{'}\left(\frac{k_1 c}{2} - d^{'}\right) \tag{15}$$

Eq. 16 recommended in ACI 318–19 [85] was used to calculate the bending moment (M_{cr}) at the first crack occurrence of the normal concrete beams. However, in order to calculate the bending moment of the beams with RWSW concrete at the time of first cracking, Eq. 17 was derived by utilising f_{sfr} suggested in Eq. 2 instead of f_r in Eq. 16. Also, y_t in Eqs. 16 and 17 represents the half length of the beams' height. In addition, I_g is the cross-sectional moment of inertia and can be calculated with Eq. 18.

$$M_{cr} = \frac{f_r I_g}{y_t} \tag{16}$$

$$M_{cr} = \frac{f_{sfr} I_g}{y_t} \tag{17}$$

$$I_g = \frac{b_w h^3}{12} \tag{18}$$

Eq. 19 proposed by Bischoff and Gross [93] for four-point loading was employed to calculate the deflection in the beams just before the first cracking. Eq. 21 was also utilised for the RWSW added specimens. The modulus of elasticity of fibreless concrete was calculated with Eq. 20 which is also recommend by ACI 318–19 [85]. The modulus of elasticity (E_{sfr}) of concrete with the RWSWs additive was calculated with Eq. 22. However, while calculating the contribution (K) of fibres to the elasticity modulus of concrete in this equation, Cox [94] mentioned that it should be multiplied by the coefficient η since the fibre additive is limited. In another study, Patton and Whittaker [95] stated that η can be taken as 0.43.

$$\delta = \frac{PL^3}{48E_c I_g}\left[3\left(\frac{a}{L}\right) - 4\left(\frac{a}{L}\right)^3\right] \tag{19}$$

$$E_c = 4700\sqrt{f_c^{'}} \tag{20}$$

$$\delta = \frac{PL^3}{48E_{sfr} I_g}\left[3\left(\frac{a}{L}\right) - 4\left(\frac{a}{L}\right)^3\right] \tag{21}$$

$$E_{sfr} = E_c\left(1 - V_f\right) + K \tag{22}$$

Table 6
Calculated RWSWs pull-out strengths and bending capacities of beams.

Test Specimens	Proposed Eq. 26			Singh [86]			ACI 544.4R-88 [87]			Campione [88]			Beshara et al. [89]		
	σ_t	$P_{Calc.}$	$\frac{P_{Calc.}}{P_{Exp.}}$	σ_t	$P_{Calc.}$	$\frac{P_{Calc.}}{P_{Exp.}}$	σ_t	$P_{Calc.}$	$\frac{P_{Calc.}}{P_{Exp.}}$	σ_t	$P_{Calc.}$	$\frac{P_{Calc.}}{P_{Exp.}}$	σ_t	$P_{Calc.}$	$\frac{P_{Calc.}}{P_{Exp.}}$
BREF-1	0.00	56.21	1.08	0.00	56.21	1.08	0.00	56.21	1.08	0.00	56.21	1.08	0.00	56.21	1.08
BTYRE-1	0.56	60.14	0.99	1.76	64.37	1.06	0.77	60.90	1.00	0.54	60.06	0.99	1.64	63.95	1.05
BTYRE-4	0.70	61.26	0.98	3.73	71.73	1.15	1.54	64.33	1.03	1.13	62.84	1.01	3.28	70.28	1.13
BTYRE-7	0.84	62.63	0.99	5.92	80.29	1.27	2.32	68.18	1.07	1.82	66.37	1.05	4.92	77.14	1.22
BREF-2	0.00	44.79	0.99	0.00	44.79	0.99	0.00	44.79	0.99	0.00	44.79	0.99	0.00	44.79	0.99
BTYRE-2	0.49	47.82	0.98	1.76	52.75	1.08	0.77	48.94	1.01	0.54	48.02	0.99	1.64	52.28	1.07
BTYRE-5	0.61	48.72	1.00	3.73	60.52	1.25	1.54	52.41	1.08	1.13	50.79	1.05	3.28	58.92	1.21
BTYRE-8	0.73	49.78	1.03	5.92	69.33	1.43	2.32	56.17	1.16	1.82	54.22	1.12	4.92	65.88	1.36
BREF-3	0.00	34.14	0.96	0.00	34.14	0.96	0.00	34.14	0.96	0.00	34.14	0.96	0.00	34.14	0.96
BTYRE-3	0.40	36.50	0.99	1.76	42.14	1.14	0.77	38.07	1.03	0.54	37.09	1.01	1.64	41.63	1.13
BTYRE-6	0.50	37.20	1.01	3.73	50.26	1.37	1.54	41.59	1.13	1.13	39.88	1.08	3.28	48.55	1.32
BTYRE-9	0.59	38.03	1.03	5.92	59.33	1.60	2.32	45.33	1.23	1.82	43.28	1.17	4.92	55.64	1.50

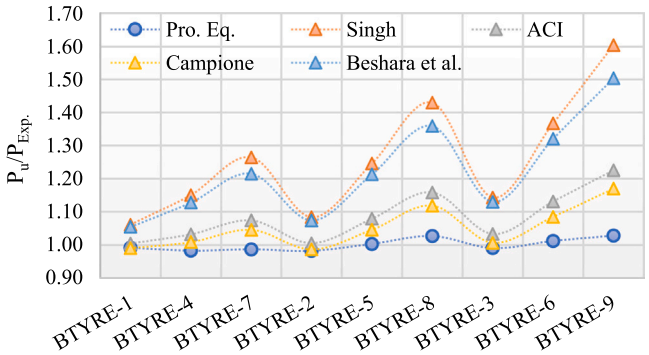

Fig. 12. Comparison of calculated bending capacities with experimental results.

$$K = \eta E_f V_f \tag{23}$$

The cracked section moment of inertia (I_{cr}) was used instead of I_g in Eq. 19 during the calculation of the deflection that occurred in the beams when the maximum bending moment acted. The values of the moment of inertia of the broken sections for the normal and RWSW reinforced concrete beams were calculated using Eqs. 24 and 25, respectively.

$$I_{cr} = \frac{b_w c^3}{3} + (n^{'} - 1)A_s^{'}(c - d^{'})^2 + A_s\left(d - c^2\right) \tag{24}$$

$$I_{cr} = \frac{b_w c^3}{3} + (n^{'} - 1)A_s^{'}(c - d^{'})^2 + (n - 1)A_s\left(d - c^2\right) + K\frac{b_w(h - c)^3}{3} \tag{25}$$

where n is the modular ratio for tension reinforcement ($n = E_s/E_c$) and n' is the modular ratio for compression reinforcement ($n'=E_s'/E_c$).

5. Pull-out strength calculation of RWSWs for RWSW concrete and determination of correction coefficient for RWSW concrete

In order to determine the pull-out stress (σ_t) that RWSWs can bear, it is necessary to determine the fibre impact coefficient (α) and fibre bond strength (τ) in Eq. 6. The bond strength of fibres is generally associated in the literature by multiplying a coefficient by the compressive stress of concrete. Further, since the effect of the reinforcement ratios on the flexural capacity was examined in this study, Eq. 6 was rearranged as Eq. 26. RWWs have an l/d ratio of 160 because the lengths and diameters of RWWs are irregular. Since the l/d ratio should be between 50 and 100 according to ACI 318–19 [85] in Eq. 26, the l/d ratio was limited to 100 in the calculations.

$$\sigma_t = \alpha(\rho - \rho^{'})V_f\frac{l}{d}\sqrt{f_{cf}^{'}} \tag{26}$$

Utilising the known bending capacities of the beams, the values of the α coefficient in Eq. 26 were determined according to the experimental results using Eqs. 14 and 15. The determined coefficients are listed in Table 5. Then, assuming that the α coefficient $(\rho\text{-}\rho')$ is related to V_f, this assumption was tested by a simple regression analysis (Fig. 11). As a result of the regression analysis, it was seen that the α coefficient was highly correlated with $(\rho\text{-}\rho')V_f$, $R^2 = 0.84$, and Eq. 27 was also generated.

$$\alpha = 0.0102\left((\rho - \rho^{'})V_f\right)^{-0.7447} \tag{27}$$

To test the usability of the shear stress (σ_t) equations for steel fibres developed by other researchers in the literature, the equations were substituted in Eq. 15, and beams' bending capacities were calculated which are given in Table 6. The l/d ratios were taken as 100 in the calculations. In addition, the results calculated with the proposed equations for the shear stress of RWSWs are presented in Table 6. The obtained results and experimental tests results are compared in Fig. 12.

Since the proposed equation in this study was optimized with the experimental results, the results calculated with this equation were very close to the experimental results (Fig. 12). There was a maximum difference of 3% between the bending capacities of the beams with RWSWs calculated by the proposed equation (Eq. 26) and the experimental results. However, there were differences up to 60% between the bending capacities calculated with the equations used for steel fibres (Eqs. 8–11) and the experimental results. This can be explained by the fact that the bond of RWSWs is lower than that of normal steel fibres. Since the diameters and lengths of RWSWs vary, the bond strength values vary too. For this reason, it is necessary to take lower adherence values for the estimation of the peel stress of RWSWs.

For the shear stress estimation of RWSWs, the bending load capacities of the beams were calculated using the proposed Eq. 26 and the derived Eqs. 12–25 (Table 6). The load-displacement curves of the calculated results from the proposed equation and experimental results are shown in Fig. 13. In the load-displacement curves obtained from the calculations using the proposed equations, the part

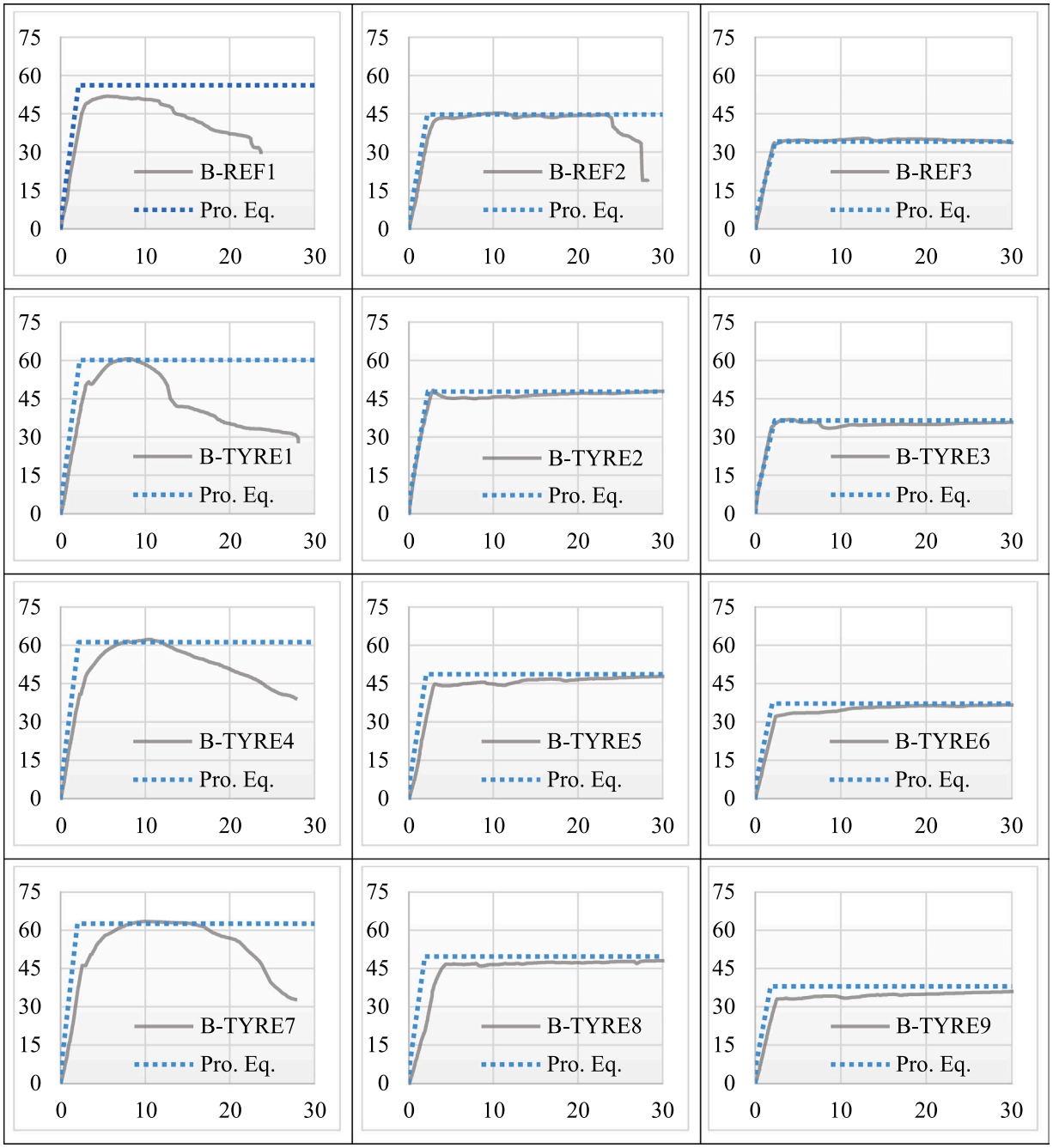

Fig. 13. Comparison of experimental and theoretical load (kN)-displacement (mm) curves.

after the yield of reinforcements is considered to be plastic. In addition, these curves were compared with the experimental ones in the figure. As can be seen from the figure, the experimental curves and theoretical curves reveal very close results. In order to determine the significance of the model, the coefficient of determination (R^2) was calculated between the experimental results and the predicted displacement results, as illustrated in Fig. 14. The clusters of points signify that the experimental data are in a good agreement with the values calculated by the proposed equation.

The model also provided high R^2 and R^2-adj correlation coefficients that vary between 97.8% and 99.9% for R^2 and 97.6% and 99.9% for R^2-adj correlation, indicating that the given quadratic model sufficiently described the experimental results.

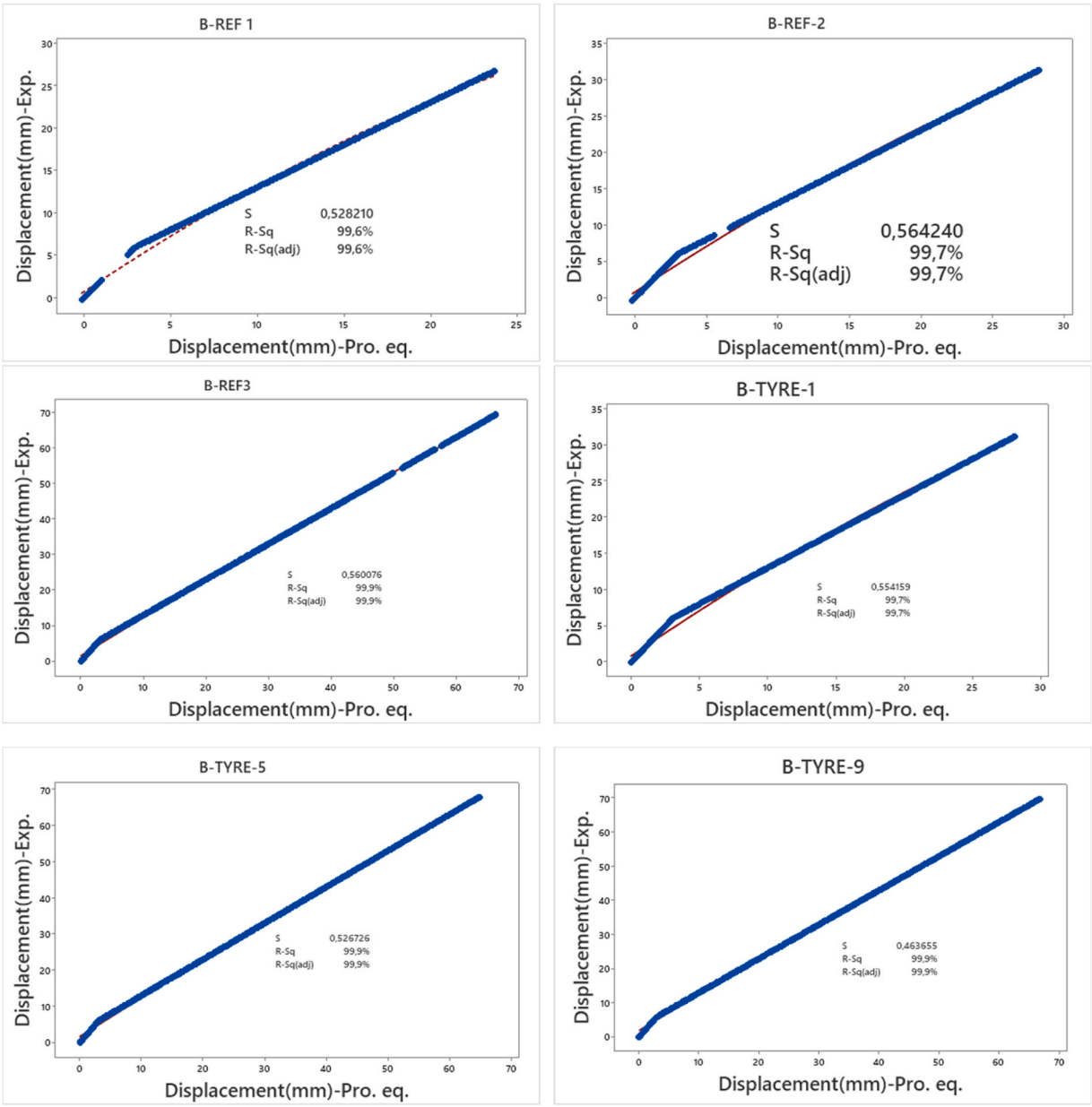

Fig. 14. Quadratic regression model of displacements (experimental results vs. calculated results).

6. Conclusions

This study analysed the bending behaviour of the reinforced concrete beams reinforced with RWSWs. The effects of the RWSWs inclusion on the failure type, energy dissipation, displacement, and ductility level were investigated. The following conclusions can be drawn:

- Up to 3% RWSWs incorporation improved the maximum and ultimate loads at similar intervals. With ϕ12 tension bar, RWSWs can be utilised effectively. RWSWs reduced the stress during the fracture initiation and propagation as load transfer elements.
- RWSWs insertion decreased the stress, while improved the ductility and energy dissipation. The elastic stage in all the beams had similar curves. Beams with 2% and 3% RWSWs displaced more than the reference beams. RWSWs significantly affected the mid-span displacements.

- The failure characteristics of BTYRE-4 and BTYRE-7 demonstrated that RWSWs in these beams could effectively bear a portion of the shear forces. Furthermore, the failure pattern of BTYRE-7 revealed that RWSWs were not uniform and certain portions of the beams fractured prematurely.
- It is suggested that a volumetric RWSW fibre dosage of 2–3% is optimal for enhancing the structural strength and safety, and decreasing the crack widths; however, reinforced concrete beams with 2% RWSWs can have a better workability.
- Comparing the findings of a similar study published in the literature [20] led to the conclusion that RWSWs are more effective than waste lathe scraps (WLSs), particularly in beams with 2ϕ10 longitudinal reinforcements. Additionally, it was found that RWSWs are more effective for the increase in the ductility demand, whereas WLS is more effective for the increase in the strength demand.
- The experimental tests results uncovered that the optimum ratio of RWSWs for the bending beams is about 2%. In future studies, it is recommended to compare the utilisation of 2% RWSWs with different parameters such as concrete compressive strength, loading, and support types.

Finally, as RWSW concrete has sufficient strength and mechanical properties compared with plain concrete, it can be concluded that RWSWs can be a reasonable choice for use as steel fibre reinforcements in structural concrete.

Declaration of Competing Interest

The authors declare that they have no known competing financial interests or personal relationships that could have appeared to influence the work reported in this paper.

Data availability

Data will be made available on request.

Acknowledgement

The authors would like to thank the Deanship of Scientific Research at Umm Al-Qura University for supporting this research work by the grant code 23UQU4250045DSR005.

References

[1] B. Zhao, G. Wang, B. Wu, X. Kong, A study on mechanical properties and permeability of steam-cured mortar with iron-copper tailings, Constr. Build. Mater. 383 (2023), 131372.
[2] Z. Qin, J. Jin, L. Liu, Y. Zhang, Y. Du, Y. Yang, et al., Reuse of soil-like material solidified by a biomass fly ash-based binder as engineering backfill material and its performance evaluation, J. Clean. Prod. 402 (2023), 136824.
[3] Y.-n Wang, Q. Wang, Y. Li, H. Wang, Y. Gao, Y. Sun, et al., Impact of incineration slag co-disposed with municipal solid waste on methane production and methanogens ecology in landfills, Bioresour. Technol. 377 (2023), 128978.
[4] Qi B., Gao S., Xu P. The Application of Recycled Epoxy Plastic Sheets Waste to Replace Concrete in Urban Construction and Building. 2023;11:201.
[5] Q. Chang, L. Liu, M.U. Farooqi, B. Thomas, Y.O. Özkılıç, Data-driven based estimation of waste-derived ceramic concrete from experimental results with its environmental assessment, J. Mater. Res. Technol. (2023).
[6] Y.O. Özkılıç, B. Başaran, C. Aksoylu, M. Karalar, C.H. Martins, Mechanical behavior in terms of shear and bending performance of reinforced concrete beam using waste fire clay as replacement of aggregate, Case Stud. Constr. Mater. 18 (2023), e02104.
[7] S. Zhou, C. Lu, X. Zhu, F. Li, Preparation and characterization of high-strength geopolymer based on BH-1 lunar soil simulant with low alkali content, Engineering 7 (2021) 1631–1645.
[8] B. Bai, F. Bai, Q. Nie, X. Jia, A high-strength red mud–fly ash geopolymer and the implications of curing temperature, Powder Technol. 416 (2023), 118242.
[9] A.İ. Çelik, U. TunÇ, A. Bahrami, M. Karalar, M.A. Othuman Mydin, T. Alomayri, et al., Use of waste glass powder toward more sustainable geopolymer concrete, J. Mater. Res. Technol. (2023).
[10] Y.O. Özkılıç, A.İ. Çelik, U. TunÇ, M. Karalar, A. Deifalla, T. Alomayri, et al., The use of crushed recycled glass for alkali activated fly ash based geopolymer concrete and prediction of its capacity, J. Mater. Res. Technol. (2023).
[11] M.C. Acar, A.İ. Çelik, R. Kayabaşı, A. Şener, N. Özdöner, Y.O. Özkılıç, Production of perlite-based-aerated geopolymer using hydrogen peroxide as eco-friendly material for energy-efficient buildings, J. Mater. Res. Technol. 24 (2023) 81–99.
[12] A.İ. Celik, Y.O. Özkılıç, Geopolymer concrete with high strength, workability and setting time using recycled steel wires and basalt powder, Steel Composite Struct. 46 (2023) 689–707.
[13] Çelik A.İ., Özkılıç Y.O., Zeybek Ö., Özdöner N., Tayeh B.A. Performance Assessment of Fiber-Reinforced Concrete Produced with Waste Lathe Fibers. 2022;14:11817.
[14] E. Madenci, S. Fayed, W. Mansour, Y.O. Ozkilic, Buckling performance of pultruded glass fiber reinforced polymer profiles infilled with waste steel fiber reinforced concrete under axial compression, Steel Composite Struct. 45 (2022) 653–663.
[15] T. Alomayri, A. Raza, F. Shaikh, Effect of nano SiO2 on mechanical properties of micro-steel fibers reinforced geopolymer composites, Ceram. Int. 47 (2021) 33444–33453.
[16] T. Alomayri, Performance evaluation of basalt fiber-reinforced geopolymer composites with various contents of nano CaCO3, Ceram. Int. 47 (2021) 29949–29959.
[17] Y. Xia, M. Shi, C. Zhang, C. Wang, X. Sang, R. Liu, et al., Analysis of flexural failure mechanism of ultraviolet cured-in-place-pipe materials for buried pipelines rehabilitation based on curing temperature monitoring, Eng. Fail. Anal. 142 (2022), 106763.
[18] Y. Huang, S. Jiang, R. Liang, Z. Liao, G. You, A green highly-effective surface flame-retardant strategy for rigid polyurethane foam: Transforming UV-cured coating into intumescent self-extinguishing layer, Compos. Part A: Appl. Sci. Manuf. 125 (2019), 105534.
[19] O.K. Djelloul, B. Menadi, G. Wardeh, S. Kenai, Performance of self-compacting concrete made with coarse and fine recycled concrete aggregates and ground granulated blast-furnace slag, Adv. Concr. Constr. 6 (2018) 103.
[20] M. Ahmadi, S. Farzin, A. Hassani, M. Motamedi, Mechanical properties of the concrete containing recycled fibers and aggregates, Constr. Build. Mater. 144 (2017) 392–398.
[21] O. Sengul, Mechanical behavior of concretes containing waste steel fibers recovered from scrap tires, Constr. Build. Mater. 122 (2016) 649–658.

[22] Y.O. Özkılıç, M. Karalar, C. Aksoylu, A.N. Beskopylny, S.A. Stel'makh, E.M. Shcherban, et al., Shear performance of reinforced expansive concrete beams utilizing aluminium waste, J. Mater. Res. Technol. 24 (2023) 5433–5448.
[23] F. Köksal, O. Gencel, B. Unal, M.Y. Durgun, Durability properties of concrete reinforced with steel-polypropylene hybrid fibers, Sci. Eng. Compos. Mater. 19 (2012) 19–27.
[24] Y. Han, S. Shao, B. Fang, T. Shi, B. Zhang, X. Wang, et al., Chloride ion penetration resistance of matrix and interfacial transition zone of multi-walled carbon nanotube-reinforced concrete, J. Build. Eng. 72 (2023), 106587.
[25] T. Alomayri, B. Ali, S.S. Raza, C. El Hachem, H. Ahmed, M. Azab, Effect of binder strengthening using micro-silica on mechanical and absorption characteristics of HPC reinforced with reclaimed jute fibres, Case Stud. Constr. Mater. 18 (2023), e02085.
[26] T. Alomayri, A. Raza, Ben, N. Kahla, Experiments and numerical simulations of glass fiber reinforced polymers in structural fibers RC members, Mech. Adv. Mater. Struct. 29 (2022) 6891–6906.
[27] Qu Zaman Khan, M.H. El Ouni, A. Raza, T. Alomayri, Mechanical behavior of electronic waste concrete columns reinforced with structural fibers and glass fiber reinforced polymer bars: Experimental and analytical investigation, Adv. Struct. Eng. 25 (2022) 374–391.
[28] Y.O. Özkılıç, C. Aksoylu, M.H. Arslan, Experimental and numerical investigations of steel fiber reinforced concrete dapped-end purlins, J. Build. Eng. 36 (2021), 102119.
[29] D. Soulioti, N. Barkoula, A. Paipetis, T. Matikas, Effects of fibre geometry and volume fraction on the flexural behaviour of steel-fibre reinforced concrete, Strain 47 (2011) e535–e541.
[30] Mehta P.K., Monteiro P.J., Concrete-Microstructure P. Materials. McGrawHill, PJM, United States. 2006:85–6.
[31] N. Banthia, M. Sappakittipakorn, Toughness enhancement in steel fiber reinforced concrete through fiber hybridization, Cem. Concr. Res. 37 (2007) 1366–1372.
[32] V.S. Gopalaratnam, R. Gettu, On the characterization of flexural toughness in fiber reinforced concretes, Cem. Concr. Compos. 17 (1995) 239–254.
[33] Nataraja M., Dhang N., Gupta A. Stress–strain curves for steel-fiber reinforced concrete under compression. Cement and concrete composites. 1999;21:383–390.
[34] A. Bonakdar, F. Babbitt, B. Mobasher, Physical and mechanical characterization of Fiber-Reinforced Aerated Concrete (FRAC), Cem. Concr. Compos. 38 (2013) 82–91.
[35] N. Buratti, B. Ferracuti, M. Savoia, Concrete crack reduction in tunnel linings by steel fibre-reinforced concretes, Constr. Build. Mater. 44 (2013) 249–259.
[36] M. Akbar, Z. Hussain, P. Huali, M. Imran, B.S. Thomas, Impact of waste crumb rubber on concrete performance incorporating silica fume and fly ash to make a sustainable low carbon concrete, Struct. Eng. Mech. 85 (2023), 000-.
[37] T.Q. Tran, B. Skariah Thomas, W. Zhang, B. Ji, S. Li, A.S. Brand, A comprehensive review on treatment methods for end-of-life tire rubber used for rubberized cementitious materials, Constr. Build. Mater. 359 (2022), 129365.
[38] B. Qi, S. Gao, P. Xu, The application of rubber aggregate-combined permeable concrete mixture in sponge city, Construction 13 (2023) 87.
[39] P.O. Awoyera, J.O. Akinmusuru, J.M. Ndambuki, Green concrete production with ceramic wastes and laterite, Constr. Build. Mater. 117 (2016) 29–36.
[40] A.M. Mhaya, G.F. Huseien, A.R.Z. Abidin, M. Ismail, Long-term mechanical and durable properties of waste tires rubber crumbs replaced GBFS modified concretes, Constr. Build. Mater. 256 (2020), 119505.
[41] B. Basaran, I. Kalkan, C. Aksoylu, Y.O. Özkılıç, M.M.S. Sabri, Effects of waste powder, fine and coarse marble aggregates on concrete compressive strength, Sustainability 14 (2022) 14388.
[42] C. Aksoylu, Y.O. Özkılıç, M. Hadzima-Nyarko, E. Işık, M.H. Arslan, Investigation on improvement in shear performance of reinforced-concrete beams produced with recycled steel wires from waste tires, Sustainability 14 (2022) 13360.
[43] M. Karalar, Y.O. Özkılıç, A.F. Deifalla, C. Aksoylu, M.H. Arslan, M. Ahmad, et al., Improvement in bending performance of reinforced concrete beams produced with waste lathe scraps, Sustainability 14 (2022) 12660.
[44] M. Karalar, Y.O. Özkılıç, C. Aksoylu, M.M.S. Sabri, A.N. Beskopylny, S.A. Stel'Makh, et al., Flexural behavior of reinforced concrete beams using waste marble powder towards application of sustainable concrete, Front Mater. 9 (2022), 1068791.
[45] T. Gönen, O. Onur, S. Cemalgil, B. Yilmazer, Y.T. Altuncu, Beton Teknolojisi İçin Yeni Atık Malzemeler Üzerine Bir İnceleme, Yapı Teknol. Elektron. Derg. 8 (2012) 36–43.
[46] A. Tiwari, S. Singh, R. Nagar, Feasibility assessment for partial replacement of fine aggregate to attain cleaner production perspective in concrete: A review, J. Clean. Prod. 135 (2016) 490–507.
[47] G. Li, M.A. Stubblefield, G. Garrick, J. Eggers, C. Abadie, B. Huang, Development of waste tire modified concrete, Cem. Concr. Res. 34 (2004) 2283–2289.
[48] F. Pelisser, N. Zavarise, T.A. Longo, A.M. Bernardin, Concrete made with recycled tire rubber: effect of alkaline activation and silica fume addition, J. Clean. Prod. 19 (2011) 757–763.
[49] A. Yilmaz, N. Degirmenci, Possibility of using waste tire rubber and fly ash with Portland cement as construction materials, Waste Manag. 29 (2009) 1541–1546.
[50] M. Bignozzi, F. Sandrolini, Tyre rubber waste recycling in self-compacting concrete, Cem. Concr. Res. 36 (2006) 735–739.
[51] Y. Wang, H. Wu, V.C. Li, Concrete reinforcement with recycled fibers, J. Mater. Civ. Eng. 12 (2000) 314–319.
[52] R. Siddique, T.R. Naik, Properties of concrete containing scrap-tire rubber–an overview, Waste Manag. 24 (2004) 563–569.
[53] X. Shu, B. Huang, Recycling of waste tire rubber in asphalt and portland cement concrete: An overview, Constr. Build. Mater. 67 (2014) 217–224.
[54] K. Neocleous, H. Tlemat, K. Pilakoutas, Design issues for concrete reinforced with steel fibers, including fibers recovered from used tires, J. Mater. Civ. Eng. 18 (2006) 677–685.
[55] M.A. Aiello, F. Leuzzi, G. Centonze, A. Maffezzoli, Use of steel fibres recovered from waste tyres as reinforcement in concrete: Pull-out behaviour, compressive and flexural strength, Waste Manag. 29 (2009) 1960–1970.
[56] J. Yang, G. Peng, G. Shui, Mechanical properties of recycled steel fiber reinforced ultra-high-performance concrete, Acta Mater. Compos. Sin. 36 (2019) 1949–1956.
[57] K. Aghaee, M.A. Yazdi, Waste steel wires modified structural lightweight concrete, Mater. Res. 17 (2014) 958–966.
[58] M.A. Köroglu, A. Ashour, Mechanical properties of self-compacting concrete with recycled bead wires, Rev. De. la Constr. 18 (2019) 501–512.
[59] Bethoft K., Samarakoon S., Evangelista L., Mikalsen B. Performance of recycled and commercial fiber reinforced concrete beams in combined action with conventional reinforcement. SynerCrete'18: Interdisciplinary Approaches for Cement-Based Materials and Structural Concrete: Synergizing Expertise and Bridging Scales of Space and Time 2018.
[60] S.S.M. Samarakoon, P. Ruben, J.W. Pedersen, L. Evangelista, Mechanical performance of concrete made of steel fibers from tire waste, Case Stud. Constr. Mater. 11 (2019), e00259.
[61] Ş. Yazıcı, G. İnan, V. Tabak, Effect of aspect ratio and volume fraction of steel fiber on the mechanical properties of SFRC, Constr. Build. Mater. 21 (2007) 1250–1253.
[62] C.D. Atiş, O. Karahan, Properties of steel fiber reinforced fly ash concrete, Constr. Build. Mater. 23 (2009) 392–399.
[63] H. Zhu, C. Li, D. Gao, L. Yang, S. Cheng, Study on mechanical properties and strength relation between cube and cylinder specimens of steel fiber reinforced concrete, Adv. Mech. Eng. 11 (2019), 1687814019842423.
[64] A. Venkateshwaran, B. Lai, J. Liew, Design of steel fiber-reinforced high-strength concrete-encased steel short columns and beams, Acids Struct. J. (2021) 118.
[65] K. Shi, M. Zhang, T. Zhang, P. Li, J. Zhu, L. Li, Seismic performance of steel fiber reinforced high–strength concrete beam–column joints, Materials 14 (2021) 3235.
[66] K. Korniejenko, M. Łach, J. Mikuła, The influence of short coir, glass and carbon fibers on the properties of composites with geopolymer matrix, Materials 14 (2021) 4599.
[67] T.F. Awolusi, O.L. Oke, O.D. Atoyebi, O.O. Akinkurolere, A.O. Sojobi, Waste tires steel fiber in concrete: A review, Innov. Infrastruct. Solut. 6 (2021) 1–12.
[68] M. Shahjalal, K. Islam, J. Rahman, K.S. Ahmed, M.R. Karim, A.M. Billah, Flexural response of fiber reinforced concrete beams with waste tires rubber and recycled aggregate, J. Clean. Prod. 278 (2021), 123842.
[69] G. Li, G. Garrick, J. Eggers, C. Abadie, M.A. Stubblefield, S.-S. Pang, Waste tire fiber modified concrete, Compos. Part B: Eng. 35 (2004) 305–312.

[70] M. Serdar, A. Baričević, M. Jelčić Rukavina, M. Pezer, D. Bjegović, N. Štirmer, Shrinkage behaviour of fibre reinforced concrete with recycled tyre polymer fibres, Int. J. Polym. Sci. 2015 (2015).
[71] A. Baričević, M.J. Rukavina, M. Pezer, N. Štirmer, Influence of recycled tire polymer fibers on concrete properties, Cem. Concr. Compos. 91 (2018) 29–41.
[72] M. Jelcic, A. Baricevic, M. Serdar, M. Grubor, Study on the post-fire properties of concrete with recycled tyre polymer fibres, Cem. Concr. Compos. (2021) 123.
[73] C. Aksoylu, Ş. Yazman, Y.O. Özkılıç, L. Gemi, M.H. Arslan, Experimental analysis of reinforced concrete shear deficient beams with circular web openings strengthened by CFRP composite, Compos. Struct. 249 (2020), 112561.
[74] S. Aykac, M. Yilmaz, Behaviour and strength of RC beams with regular triangular or circular web openings, J. Fac. Eng. Archit. Gazi Univ. (2011) 26.
[75] M. Najafgholipour, S. Dehghan, A. Dooshabi, A. Niroomandi, Finite element analysis of reinforced concrete beam-column connections with governing joint shear failure mode, Lat. Am. J. Solids Struct. 14 (2017) 1200–1225.
[76] K. Kawamura, H. Nakamura, M. Takemura, T. Miura, Analytical study on the effect of different shear reinforcement shapes on shear failure behavior and shear resistance mechanism of RC beams, J. Adv. Concr. Technol. 19 (2021) 571–584.
[77] B. Piscesa, H. Alrasyid, D. Prasetya, Numerical investigation of reinforced concrete beam due to shear failure, IPTEK J. Technol. Sci. 31 (2021) 373–382.
[78] A. Bhutti, N. Kishi, H. Mikani, T. Ando, Elasto-plastic impact analysis of shear-failure-type RC beams with shear rebars, Mater. Des. 30 (2009) 502–510.
[79] G. Radaelli, J.L. Herder, Shape optimization and sensitivity of compliant beams for prescribed load-displacement response, Mech. Sci. 7 (2016) 219–232.
[80] A. Maryoto, N.I.S. Hermanto, Waste tire application in concrete structures, Aceh Int. J. Sci. Technol. 6 (2017) 8–18.
[81] M. Sienkiewicz, H. Janik, K. Borzędowska-Labuda, J. Kucińska-Lipka, Environmentally friendly polymer-rubber composites obtained from waste tyres: A review, J. Clean. Prod. 147 (2017) 560–571.
[82] R. Roychand, R.J. Gravina, Y. Zhuge, X. Ma, O. Youssf, J.E. Mills, A comprehensive review on the mechanical properties of waste tire rubber concrete, Constr. Build. Mater. 237 (2020), 117651.
[83] C. Shi, Y.-L. Mo, High-Performance Construction Materials: Science and Applications, World scientific,, 2008.
[84] R. Swany, P. Mangat, A theory of flexural strengh of steel-fibre reinforced composite, Cem. Concr. Res 4 (1974) 313–320.
[85] A. Committee. Building Code Requirements for Structural Concrete and Commentary (ACI 318-19), American Concrete Institute, Farmington Hills, MI, USA, 2019, p. 623.
[86] H. Singh, Flexural modeling of steel fiber-reinforced concrete members: analytical investigations. Practice Periodical on Structural Design and Construction 20 (2015), 04014046.
[87] ACI 544.4R-88, Design Considerations for Steel Fiber Reinforced Concrete, American Concrete Institute,, MI, USA, 1999.
[88] G. Campione, Simplified flexural response of steel fiber-reinforced concrete beams, J. Mater. Civ. Eng. 20 (2008) 283–293.
[89] F. Beshara, I. Shaaban, T. Mustafa, Nominal flexural strength of high strength fiber reinforced concrete beams, Arab. J. Sci. Eng. 37 (2012) 291–301.
[90] G. Campione, L. La Mendola, M. Papia, Shear strength of steel fiber reinforced concrete beams with stirrups, Struct. Eng. Mech. Int. J. 24 (2006) 107–136.
[91] H. Singh, Steel Fiber Reinforced Concrete: Behavior, Modelling and Design, Springer, 2016.
[92] R.B. Abdul-Ahad, O.Q. Aziz, Flexural strength of reinforced concrete T-beams with steel fibers, Cem. Concr. Compos. 21 (1999) 263–268.
[93] P.H. Bischoff, S.P. Gross, Equivalent moment of inertia based on integration of curvature, J. Compos. Constr. 15 (2011) 263–273.
[94] H. Cox, The elasticity and strength of paper and other fibrous materials, Br. J. Appl. Phys. 3 (1952) 72.
[95] M.E. Patton, W. Whittaker, Effects of fiber content and damaging load on steel fiber reinforced concrete stiffness, J. Proc. (1983) 13–16.